Supporting Information

Theoretical Design of Rhombohedral-Stacked MoS_2-Based Ferroelectric Tunneling Junctions with Ultra-High Tunneling Electroresistances

Huamin Hu[1], Guang Zeng[1*], and Gang Ouyang[2*]

[1]*School of Materials Science and Engineering, Changsha University of Science and Technology, Changsha 410114, China*

[2]*Key Laboratory of Low-Dimensional Quantum Structures and Quantum Control of Ministry of Education, School of Physics and Electronics, Hunan Normal University, Changsha 410081, China*

*Corresponding authors. E-mail: zengguang@csust.edu.cn (G. Zeng), gangouy@hunnu.edu.cn (G. Ouyang)

Figure S1

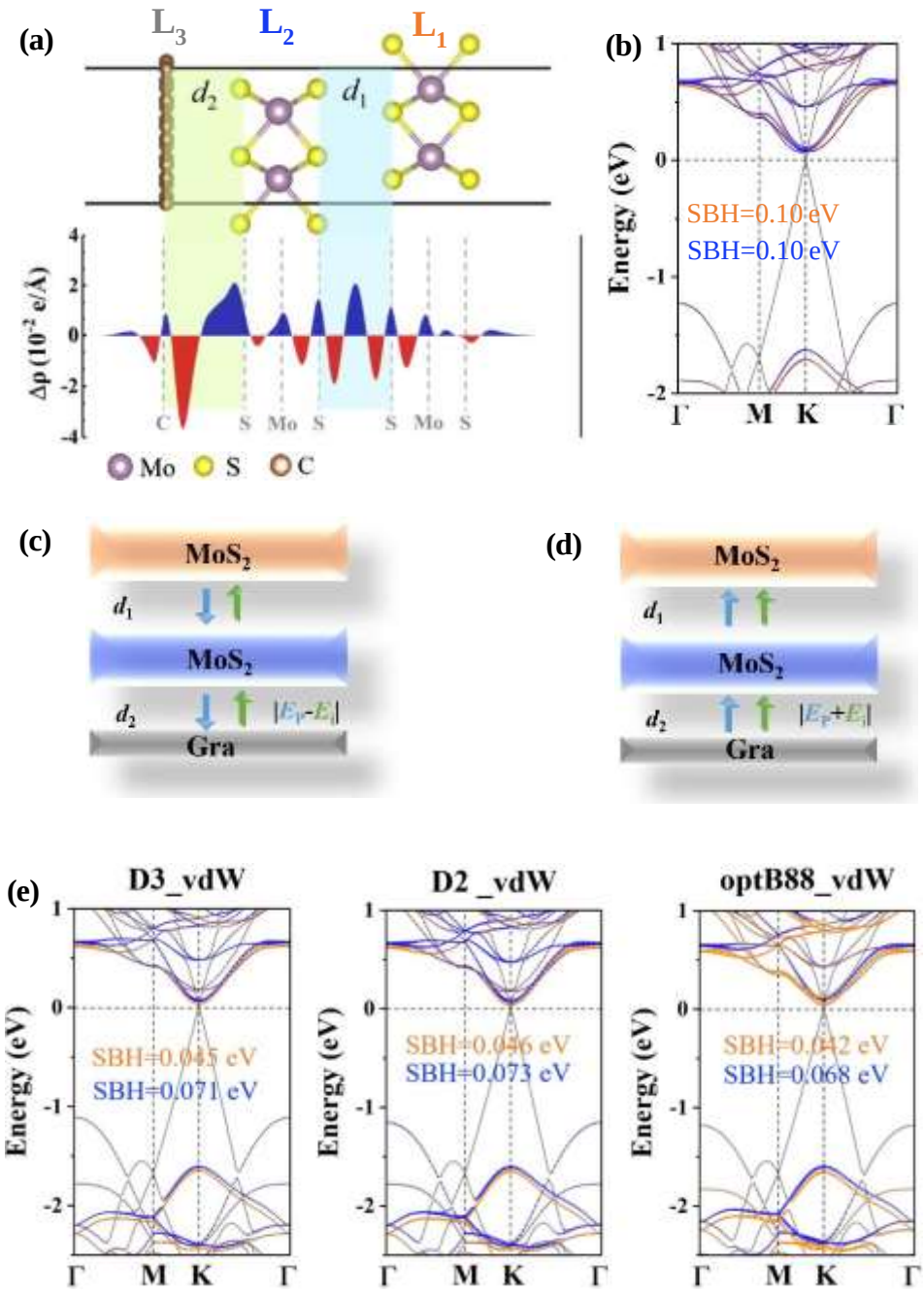

Figure S1. (a) Atomic structure, differential charge density and (b) band structure of Gra/2H-MoS_2. (c, d) Schematic of the interaction between the ferroelectric polarized electric field (E_p) and the built-in electric field (E_i). (e) Band structure of Gra/2R-MoS_2 P↑ with D3, D2, and optB88 vdW correction.

Figure S2

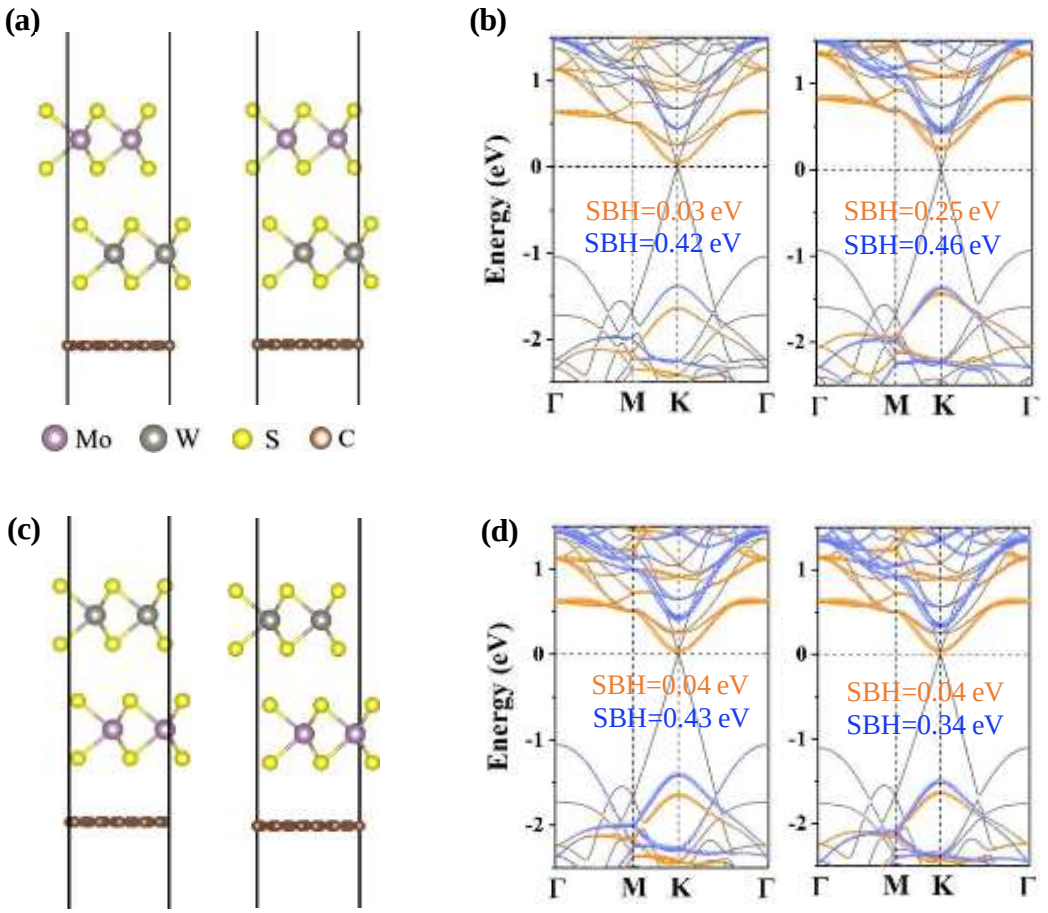

Figure S2. Atomic structures and band structures of Gra/WS_2/MoS_2 (a, b), as well as Gra/MoS_2/WS_2 (c, d).

Figure S3

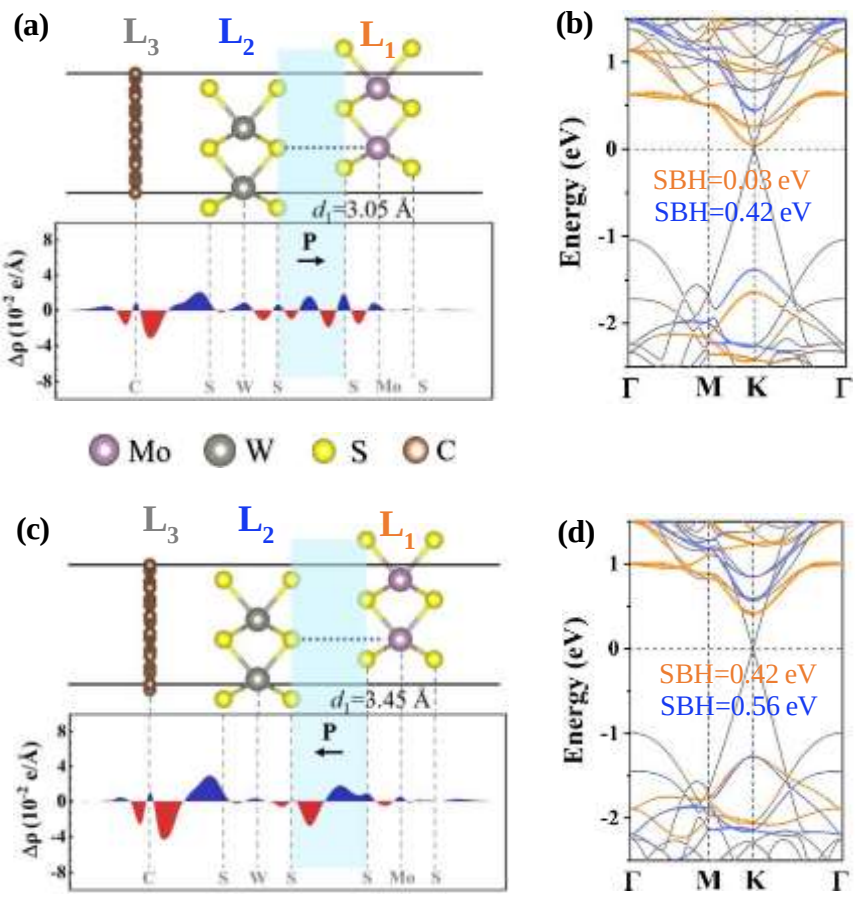

Figure S3. Planar differential charge density (a, c) and band structure (b, d) of Gra/WS_2/MoS_2 P↑ state.

Figure S4

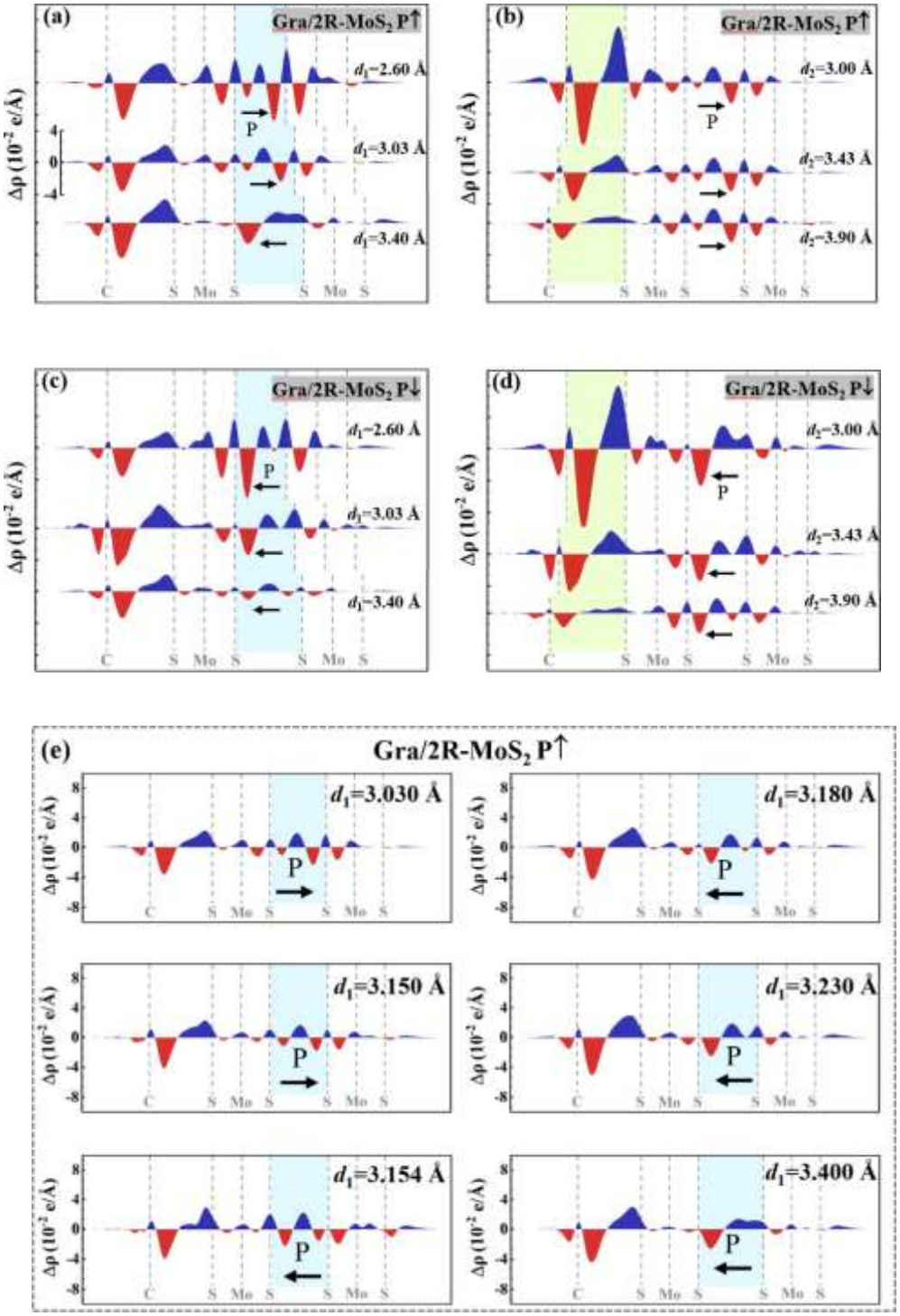

Figure S4. Planar differential charge density of Gra/2R-MoS_2 in (a-b) P↑ and (c-d) P↓ with different interface distances (d_1 and d_2). (e) interfacial polarization direction of 2R-MoS_2 reverses when d_1 increases by 0.124 Å.

Figure. S5

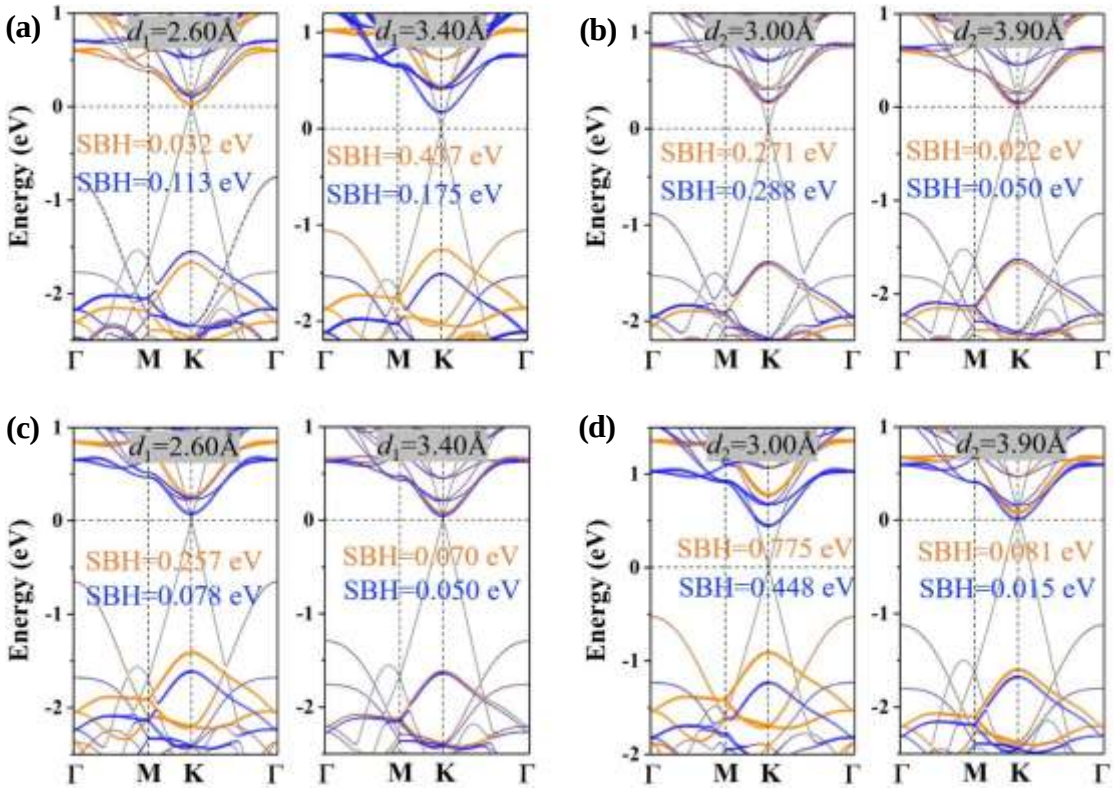

Figure. S5. Electron band structures of (a-b) Gra/2R-MoS_2 P↑ and (c-d) Gra/2R-MoS_2 P↓ with different interface distances d_1 and d_2.

Figure S6

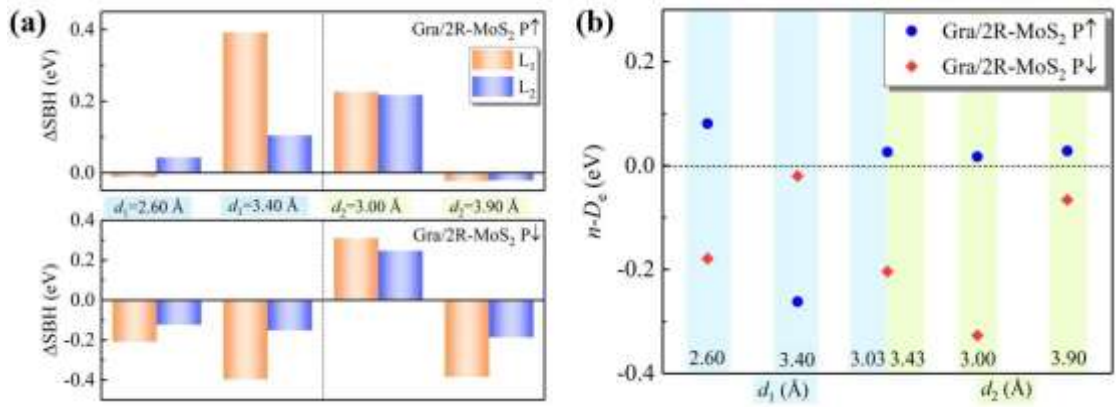

Figure S6. (a) The SBH of L_1 and L_2 in Gra/2R-MoS_2 changes as d_1 and d_2 are adjusted. (b) band non-degeneracy (n-D_e) of 2R-MoS_2 in Gra/2R-MoS_2 heterojunction with different d_1 and d_2.

Figure. S7

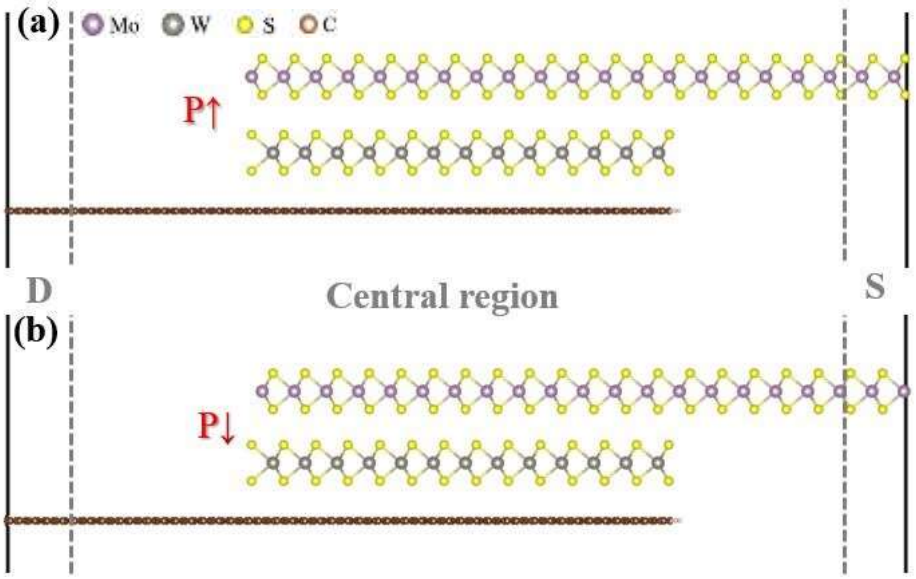

Figure S7. Device configurations in the DFT+NEGF calculations for 2D vdW (a) Gra/2R-MoS_2 P↑ and (b) Gra/2R-MoS_2 P↓ states. A vacuum padding of 10Å is set along the vertical direction in order to eliminate any interlayer coupling effect. The transmission intensity is indicated in logarithmic scale by color bar and the electron transmission coefficients are in Table 2.

Figure S8

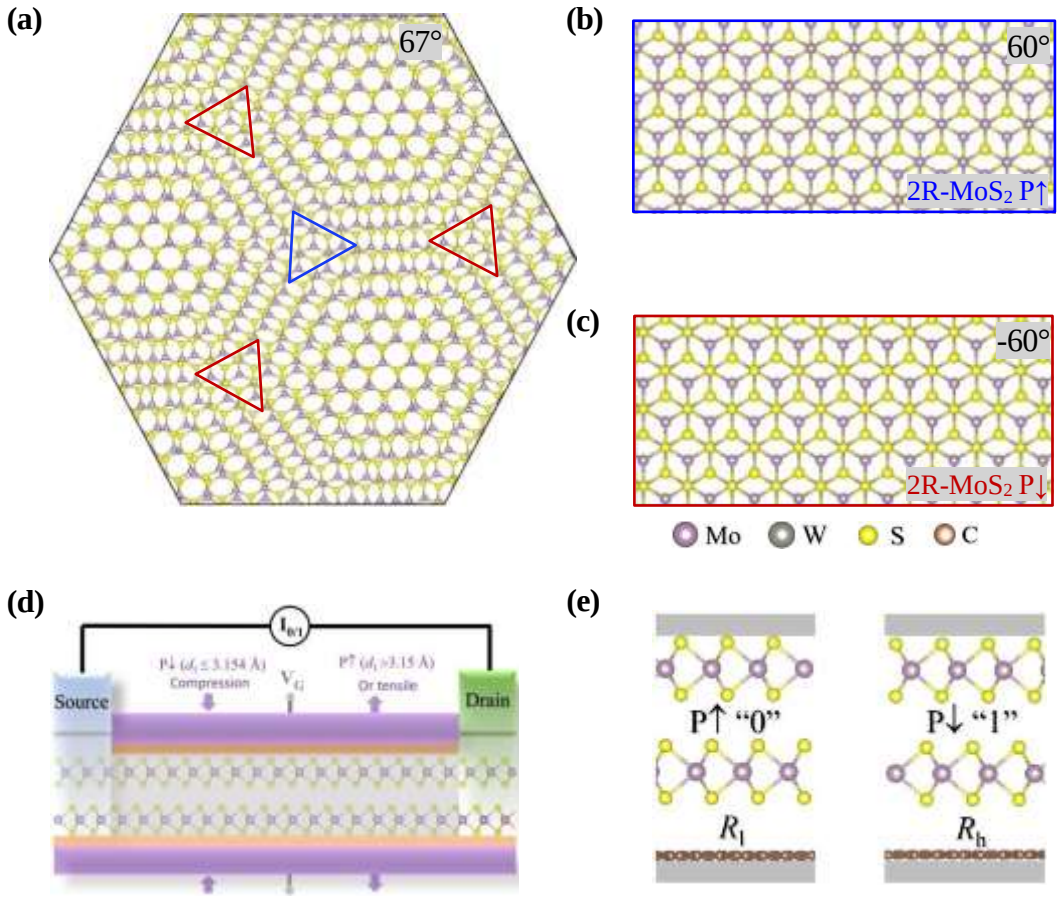

Figure S8. The moiré superlattice structure is obtained by twisting (a) 67°, (b) 60°, and (c) -60° in 2H-MoS_2 plane direction, where blue and red triangles represent 2R-MoS_2 P↑ and 2R-MoS_2 P↓, respectively. (d) Field-effect transistor and (e) memory logic unit diagram for Gra/2R-MoS_2, where the purple arrow indicates the direction of the stress. R_l and R_h denote low and high resistance contacts, respectively.

Figure S9

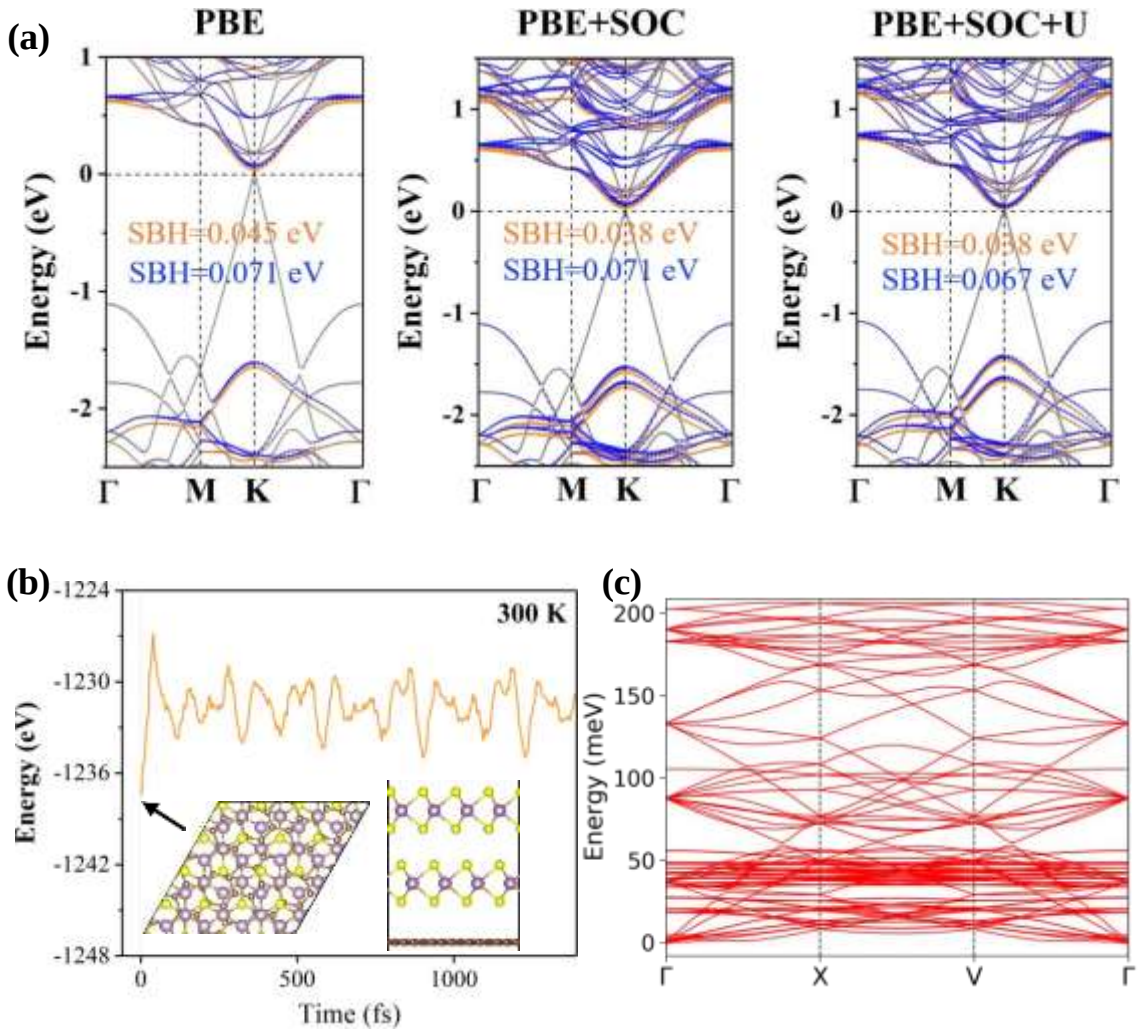

Figure S9. (a) Band structure of Gra/2R-MoS_2 P↑ with PBE, PBE+SOC, and PBE+SOC+U_{eff} (U_{eff} = 4 eV). (b) Molecular dynamics of 2×2×1 supercell Gra/2R-MoS_2 P↑. (c) Phonon band structure of Gra/2R-MoS_2 P↑.

Figure S10

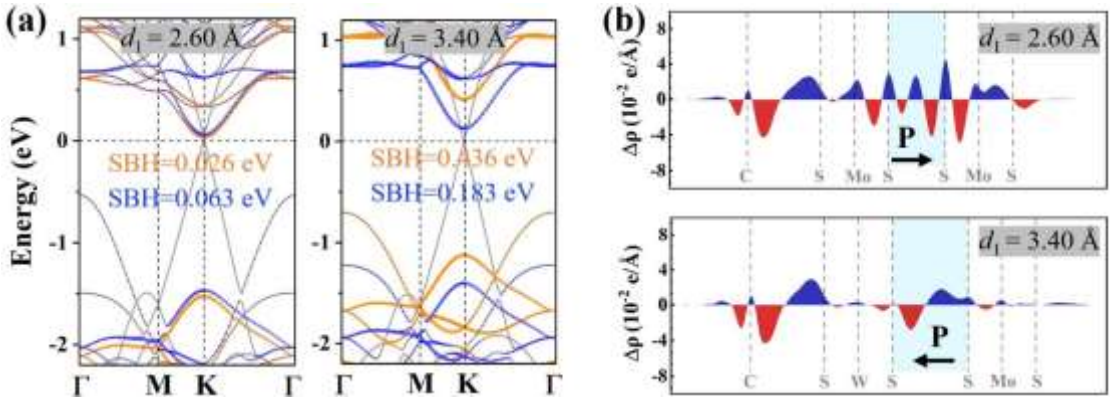

Figure S10. Band structure (a) and planar differential charge density (b) of Gra/2R-MoS_2 P↑ with different interface distances d_1, in which the atoms, lattice and volume have been optimized simultaneously.

Table S1. Optimized lattice constant (*a* and *b*), lattice angle (α/β/γ), and lattice mismatch rate (*η*) of systems.

Systems	*a* (Å)	*b* (Å)	α/β/γ	*η*
Gra/2H-MoS_2	6.32	6.32	90°/90°/60°	1.3%
Gra/2R-MoS_2	6.36	6.36	90°/90°/60°	1.3%
Gra/R-MoS_2/WS_2	6.36	6.36	90°/90°/60°	1.3%
2R-MoS_2/h-BN	6.49	6.49	90°/90°/60°	2.1%
2R-MoS_2/Au	11.27	18.63	90°/90°/90°	2.3%
2R-MoS_2/Si	13.00	13.00	90°/90°/60°	2.3%